URSI AP-RASC 2019, New Delhi, India, 09 - 15 March 2019

Mode Analysis and Design of PBG Cavity for Tunable Gyrotron

Rajanish Kumar Singh, M. Thottappan
Department of Electronics Engineering
Indian Institute of Technology (BHU), Varanasi-221005, INDIA
rajanishks.rs.ece15@iitbhu.ac.in, mthottappan.ece@iitbhu.ac.in

Abstract

A Metal Photonic-band-gap (MPBG) cavity is designed and simulated to operate in $TE_{15,3}$ mode for second harmonic tunable gyrotron. The ADI-FDTD algorithm is used to investigate a unit cell of triangular metal PBG structure. The dispersion and global band diagram have been plotted for unit cell of triangular PBG structure. The MPBG cavity is formed by creating a defect in the 2-D periodic triangular PBG structure. The mode analysis has been done to estimate the all possible mode those can confine in the defect of periodic MPBG structure. The MPBG cavity has been modeled and simulated to observe its propagation behavior using a commercial 3D electromagnetic code. The return loss of the cavity is observed as ~47.62dB through its transient analysis. Its quality factor is observed as ~13143 through its Eigenmode analysis for the desire $TE_{15,3}$ mode at ~527.5GHz.

1. Introduction

Gyrotrons proved itself as a very efficient source of power in microwave frequency and THz regime. Its application is not only in electron cyclotron heating, communication (radar), plasma diagnostics but also in DNP / NMR spectroscopy [1, 2]. DNP is a technique that increases the intensity of signals in NMR experiments. Recently, DNP/NMR spectroscopy is the most advance technique to predict the nature of biological samples, protein structure due to its magnificent resolution in NMR spectra. To attain better spectral resolution in NMR spectroscopy, NMR experiment needs higher magnetic field that pushes the gyrotron to operate at higher operating frequencies. Propitiously, some gyrotrons in THz regime are available now to fulfill the demand of DNP/NMR experiments [3, 4]. Obviously, when operating frequency increases then transverse dimension of RF circuit reduces as well this leads the reduction in interaction efficiency and also increases the complexity in its fabrication. These problems can be alleviated by using overmoded structures, but the conventional cavities are suffered by the problem of mode competition [5]. To overcome the problem of mode competition, RF circuit should be mode selective with high mode purity. The Photonic-Band-Gap cavity is successfully demonstrated itself as a frequency selective and mode selective. The PBG structures are basically periodic lattice of metal rods, dielectric rods or amalgamation of both metal and dielectric rods. It can be 1D, 2D or 3D structure however; the 2D PBG structure is generally used because 2D PBG structures are invariant along the longitudinal axis and periodic in transverse plane. The PBG structure is non-transparent for a particular frequency range namely stop band and transparent to the rest frequency range namely passband in the electromagnetic (EM) spectrum. The PBG cavity has prospective application in millimeter and sub-millimeter regime devices like antenna, microwave filters, planar reflectors, etc. [6]. PBG structures also find application in the vacuum electronics devices (VED) including gyrotron oscillator, backward wave oscillator (BWO), gyro-TWT, and accelerator.

In the present work, a sub-millimeter wave gyrotron cavity using metal PBG structure operating in $TE_{15,3}$ mode at ~527GHz is presented. The aim of the MPBG cavity to attain high mode purity as well wide tunable bandwidth for THz gyrotron as it is needed for DNP/NMR spectroscopy applications.

2. Design, Modelling and Mode Analysis

The PBG structures are mainly two type's triangular lattice structure and square lattice structure. The triangular lattice (Fig. 1) of PBG structure is chosen over square lattice of PBG structure because it's have better azimuthal symmetry. The periodic structure and irreducible brillouin's zone (shaded region) of PBG has been shown in Fig. 1(a) and (b), where 'r' and 'a' are rod radius and lattice constant, respectively. The reciprocal lattice has three symmetric points [Fig. 1(b)] namely Γ, X and M. The dispersion relation of PBG structure is calculated by using ADI-FDTD algorithm. The ADI-FDTD method has considerable advantage as compare to other established implicit type methods because it's have magnificent ability to solve the multi-dimensional problems [7]. The dispersion relation for TE modes of PBG structure [Fig. 2(a)] is calculated by Eigenvalues of the wave vector by following the path as Γ-X, X-M and M-Γ of (shaded region) brillouin's zone. The global band gap [Fig. 2(b)] is obtained by observing the band gap in dispersion relation for range of 0 to 0.5 of *r/a*.

To impound the desire mode and wipe out its nearby modes, the operating point [● of Fig. 2(b)] must be chosen in global band diagram. A defect is created in such a way that the defect radius is approximately equal to required radius to confine the desire mode within it. The defect of the PBG structure acts as a RF interaction circuit, in which electron beam interacts to the RF wave. The radius of the cylindrical cavity with the resonant frequency 'f' is given by [1],

$$R = \frac{cx'_{mn}}{2\pi f} \tag{1}$$

Where, x'_{mn} is the n^{th} zero roots of the m^{th}-order Bessel function $J'_m(x)$. To confine the operating mode in the defect, the radius of the defect after removing certain number of metallic rods must be close to the required radius of the cylindrical cavity. The defect radius (R) after removing seven rods and nineteen rods form the triangular PBG structure are given by $R = \sqrt{3}a - r$ and $R = \sqrt{7}a - r$, respectively, where 'r' is the rod radius and 'a' is lattice constant. Therefore, we have [8],

$$fa/c = \begin{cases} x'_{mn} \big/ 2\pi\left(\sqrt{3} - r/a\right) \\ x'_{mn} \big/ 2\pi\left(\sqrt{7} - r/a\right). \end{cases} \tag{2}$$

Where, 'f', 'a', 'r' and 'c' are the confined frequency, lattice constant, rod radius and velocity of light, respectively. The possible confined EM modes as shown in Figs. 3(a) and 3(b) (for the removal of nineteen rods) are obtained by using equations (1) and (2), and global band gap diagram. It is observed that mode competition is considerably reduced because operating mode lies in the band gap and other modes lie in pass band. The defect (PBG cavity) is perceived by unfastening nineteen rods from the PBG structure to confine the desired $TE_{15,3}$ operating mode.

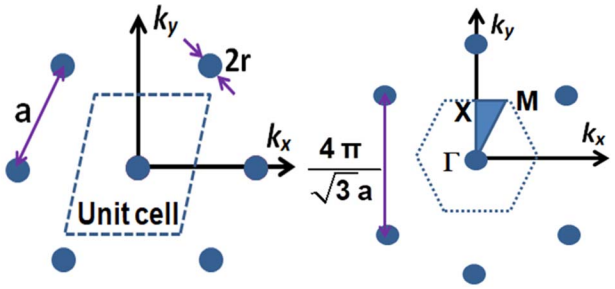

(a) (b)

Figure 1. (a) Triangular lattice of MPBG structure, (b) reciprocal lattice with brillouin's zone (shaded region) of MPBG structure.

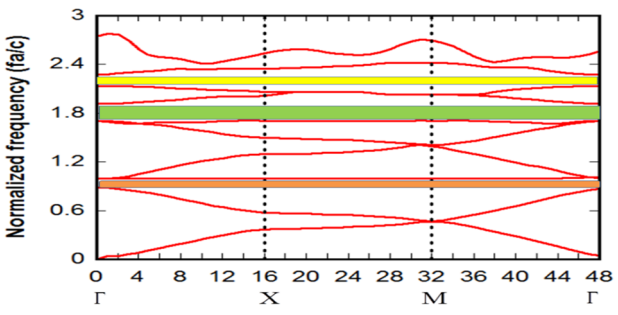

(a)

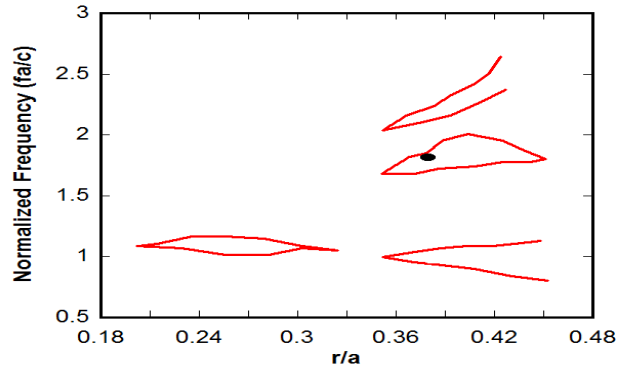

(b)

Figure 2. (a) Dispersion relation of a triangular MPBG structure, (b) Global band diagram, where ● is the operating point [6].

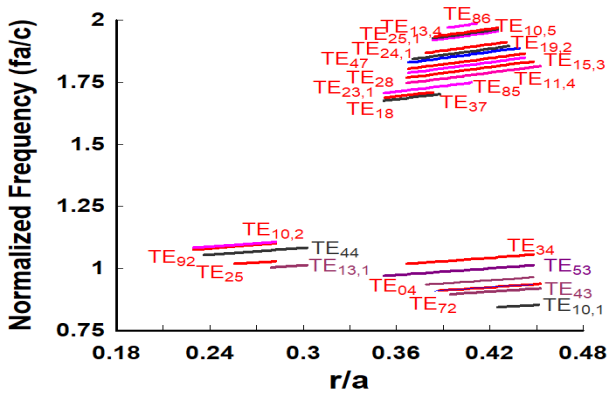

(a)

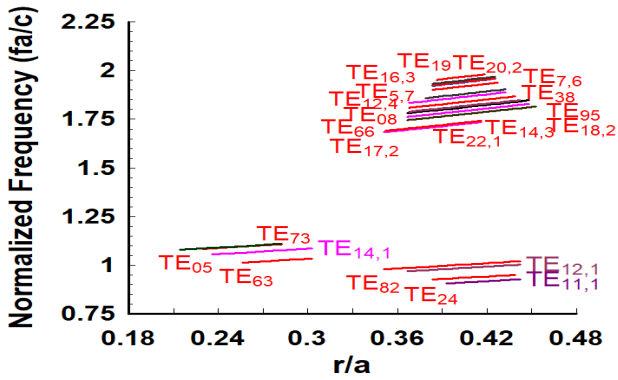

(b)

Figure 3. (a) & (b) Relation between r/a and fa/c of different modes those confine in the defect after removing nineteen rods.

In the present design, chosen operating points [Fig. 2(b)] are as fa/c = 1.86, and r/a = 0.39. The design parameters of the PBG cavity are given in Table - I.

TABLE I: Design parameters of PBG cavity

Operating Frequency (GHz)	Operating Mode	Lattice Constant 'a' (mm)	Rod Radius 'r' (mm)	PBG Cavity Radius (mm)
527	$TE_{15,3}$	1.06	0.41	11.48

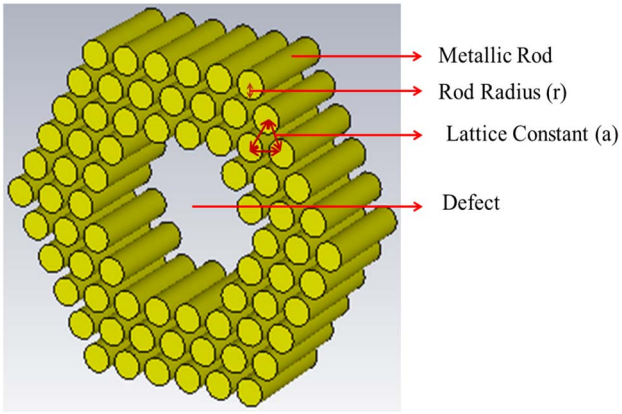

Figure 4. Model of designed PBG cavity.

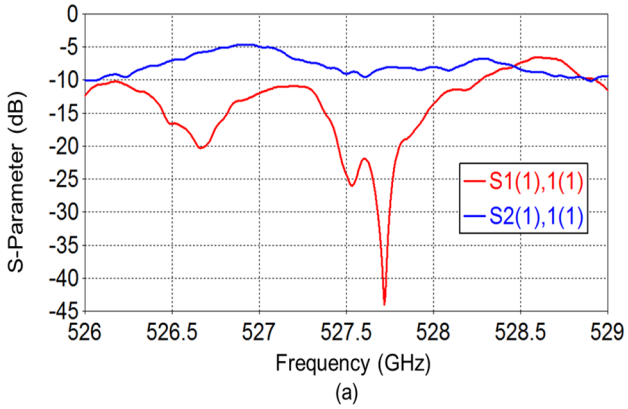

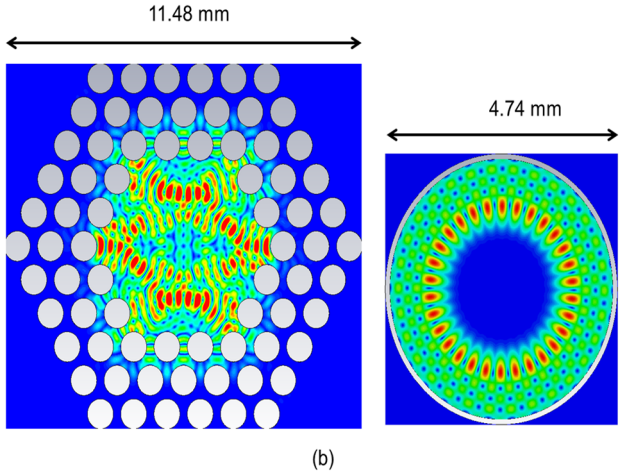

Figure 5. (a) Diagram of S-Parameter, (b) E-field pattern of $TE_{15,3}$-like mode in the PBG cavity and $TE_{15,3}$ mode in the cylindrical cavity.

TABLE II

Mode	Conventional Cavity		PBG Cavity	
	Res. Freq. (GHz)	Ohmic Q	Res. Freq. (GHz)	Ohmic Q
$TE_{2,8}$	520.75	25132	523.97	4649
$TE_{0,8}$	521.72	25320	518.49	7643
$TE_{15,3}$	527.24	17202	527.56	13143
$TE_{12,4}$	528.62	20231	528.09	8774

3. Results and Discussion

The PBG cavity is modeled in "CST Microwave Studio" as shown in Fig. 4. The S-parameters for the simulated PBG cavity is shown in Fig. 5(a). The S_{11} (reflection coefficient) is obtained as -43.95dB and S_{21} (transmission coefficient) is obtained as -8.18dB at ~527.70GHz. The quality factor of the confined modes is calculated for both PBG cavity and analogous conventional cavity using Eigenmode simulation. The quality factor of operating $TE_{15,3}$ like mode and other competing modes are shown in Table- II. The Fig. 5(b) shows the E-field pattern of confined $TE_{15,3}$–like mode. The quality factor (Q) of $TE_{15,3}$ –like mode is observed higher than nearby modes like $TE_{12,4}$, $TE_{2,8}$ and $TE_{0,8}$ as given in Table-II. The Q factor of $TE_{15,3}$-like mode is obtained as ~13143 at ~527.56GHz. An analogous conventional cavity is also simulated to observe the quality factors of $TE_{15,3}$ and other competing modes. The Q factor of $TE_{15,3}$ mode is found as ~17206, which is higher than obtained quality factor for PBG cavity but lower than other competing modes. So PBG cavity suppressed the competing modes, which are required in higher order operating modes. The contour plot of $TE_{15,3}$ mode is shown in Fig. 5(b).

4. Conclusion

A MPBG cavity has been designed and modeled to operate in $TE_{15,3}$ -like mode for 527GHz gyrotron oscillator. The reflection (S_{11}) and transmission (S_{21}) coefficients of the cavity were found to be minimum and maximum, respectively at ~527.7GHz. The quality factor concerned with the desired operating $TE_{15,3}$-like mode has been calculated as ~13143 which is good enough for its confinement in the PBG cavity (defect) at ~527GHz. This ensures that the single mode operation. Further, fabrication difficulties were also reduced by using PBG cavity because transverse dimension of MPBG cavity is sufficiently large at such high operating frequencies.

5. References

1. M. V. Kartikeyan, E. Borie, and M. Thumm, "Gyrotrons-High Power Microwave and Millimeter Wave Technology," Berlin, Germany: Springer-Verlag, 2004.
2. E. Nanni, R. G. Griffin, "THz Dynamic Nuclear Polarization NMR," IEEE Trans. THz Sci. and Technl., 2011, pp. 145–163, DOI: 10.1109/TTHZ.2011.2159546.
3. T. Idehara, I. Ogawa, L. Agusu, T. Kanemaki, S. Mitsudo, T. Saito, T. Fujiwara, and H. Takahashi, "Development of 394.6 GHz CW gyrotron (gyrotron FU CW II) for DNP/proton-NMR at 600 MHz," Int. J. Infrared Millim. Waves, vol. 28, April, 2007, pp. 433–442, DOI 10.1007/s10762-007-9224-x.
4. K. Kreischer, C. Farrar, R. Griffin, R. Temkin, and J. Vieregg, "250 GHz gyrotron for NMR spectroscopy," in Proc. IEEE 27th Int. Conf. on Plasma Science, New

Orleans, LA, , June, 2000, pp. 198, DOI: 10.1109/PLASMA.2000.854998 .
5. G.P. Saraph, T.M. Antonsen, B. Levush and G.I. Lin, “Regions of stability of high-power gyrotron Oscillators,” IEEE Trans. Plasma Sci., vol. 20, June 1992, pp. 115-125, DOI: 10.1109/27.142810.
6. J. R. Sirigiri., K. E. Kreischer, J. Macuhzak, I. Mastovsky, M. A. Shapiro, and R. J. Temkin, “Photonic band gap resonator gyrotron,” Phys. Rev. Lett., vol. 86, 2001, pp. 5628-5631, doi.org/10.1103/ PhysRevLett.86.5628 .
7. M.Qiu and S. He, “A nonorthogonal finite-difference time-domain method for computing the band structure of a two-dimensional photonic crystal with dielectric and metallic inclusions,” J. Appl. Phys., vol. 87, no. 12, June, 2000, pp. 8268–8275, doi.org/10.1063/1.373537.
8. Yanyan Zhang, Sheng Yu, Liang Zhang, Tianzhong Zhang, Youwei Yang, and Hongfu Li, “Analysis of the photonic bandgaps for gyrotron devices ,” IEEE Trans. Plasma Sci., vol. 43, no. 4, April 2015, pp. 1018-1023, DOI: 10.1109/TPS.2015.2411286.